EPJ Web of Conferences **29**, 00051 (2012)
DOI: 10.1051/epjconf/20122900051
© Owned by the authors, published by EDP Sciences, 2012

Structural, magnetic and magnetocaloric properties of $Pr_{0.6-x}Er_xSr_{0.4}MnO_3$ (x = 0.0, 0.1 and 0.2)

R. M'nassri[1,2], W. Cheikhrouhou-Koubaa[1], N. Boudjada[2] and A. Cheikhrouhou[1,2,a]

[1] Laboratoire de Physique des Matériaux, Faculté des Sciences de Sfax, Sfax University, B.P. 1171, 3000 Sfax, Tunisia
[2] Institut NEEL, B.P. 166, 38042 Grenoble Cedex 9, France

Abstract. We investigate the effect of Erbium doping on the structural, magnetic and magnetocaloric properties of $Pr_{0.6-x}Er_xSr_{0.4}MnO_3$ (x = 0.0, 0.1 and 0.2) powder samples. Our polycrystalline samples were synthesized using the solid-state reaction at high temperature. X-ray diffraction characterizations showed that all our studied samples crystallize in the distorted orthorhombic system with Pnma space group. All our synthesized samples exhibit a paramagnetic–ferromagnetic transition with decreasing temperature. The magnetic transition temperature T_C is found to decrease continuously with increasing Er concentration. It was found that the maximum value of the magnetic entropy change for $Pr_{0.4}Er_{0.2}Sr_{0.4}MnO_3$ sample reached $\left|\Delta S_M^{max}\right|$ = 2.40 J $kg^{-1}K^{-1}$ in a magnetic applied filed of 2T.

1 Introduction

Presence of well-defined crystallographic and magnetic sublattices within the same compound usually leads to very interesting phenomena in reason of the strong interplay between localized moments, itinerant electrons, magnetic order, and other important features which characterize each one of the competing phases. In the recent years manganites with general formula of $Ln_{1-x}M_xMnO_3$ (Ln=rare-earth element and M=divalent metal such as Ca, Sr, Ba, etc.) have been elaborated and studied [1] in order to understand their mechanism of transport and spin ordering. The perovskite structure generally shows lattice distortion as modifications from the cubic system to rhombohedral or orthorhombic one mainly due to the Jahn–Teller (JT) effect causing the deformation of the MnO_6 octahedra. The double exchange theory and the Jahn–Teller effect were used to understand the ferromagnetic–paramagnetic (FM–PM) phase transition associated with an insulator–metal (IM) one in the manganites [2,3], thus giving rise to the well known colossal magnetoresistance (CMR) [1].

$Pr_{1-x}Sr_xMnO_3$ perovskite manganite is an important member in the manganite family with intermediate one electron bandwidth [4]. The Pr-based manganites show many novel properties including the charge ordering (CO) state, FM and antiferromagnetic (AFM) coexistence and metamagnetic transition [5-7]. For $x < 0.5$, it possesses a strong ferromagnetic–paramagnetic (FM–PM) transition and a large magnetoresistance effect. As $x \geq 0.5$, it shows a CO-antiferromagnetic

[a] e-mail : abdcheikhrouhou@yahoo.fr

This is an Open Access article distributed under the terms of the Creative Commons Attribution License 2.0, which permits unrestricted use, distribution, and reproduction in any medium, provided the original work is properly cited.

Article available at http://www.epj-conferences.org or http://dx.doi.org/10.1051/epjconf/20122900051

(AF) state. In this paper, we investigate the magnetocaloric effect (MCE) in the $Pr_{0.6-x}Er_xSr_{0.4}MnO_3$ which may be possess potential applications in magnetic refrigeration technology.
The influence of Er-doping on the ground state and the evolution of field dependent phase transition has been discussed. Er-doping at Pr-site results in an average $\langle r_A \rangle$ ~1.208 Å for x= 0.2, compared to $\langle r_A \rangle$~1.231Å in the parent compound $Pr_{0.6}Sr_{0.4}MnO_3$ (PSMO). The A-site disorder, $\sigma_A^2 \sim 8.76.10^{-3}$Å^2 for x=0.2, compared to $\sigma_A^2 \sim 4.118.10^{-3}$Å^2 for PSMO signifies the huge disorder in our system.

2 Experimental techniques

Polycrystalline $Pr_{0.6-x}$ $Er_xSr_{0.4}MnO_3$ samples were prepared using the conventional ceramic route at high temperature. The precursors Pr_6O_{11}, $SrCO_3$, Er_2O_3 and MnO_2 with purity more than 99% were intimately mixed in an agate mortar and then heated in air up to 1000°C for 60 h. The obtained powders were pressed into pellets (of about 1mm thickness) and sintered at 1350°C in air for 60 h with intermediate regrinding and repelling. Finally, these pellets were cooled slowly to room temperature in air. Phase purity, homogeneity and cell dimensions were determined by X-ray powder diffraction (XRD) at room temperature (diffractometer using Cu Kα radiation). Structural analysis was carried out using the standard Rietveld method [8, 9]. Magnetization (M) versus temperature (T) in the range 20–300K under 0.05T and versus magnetic applied field (H) up to 7T at several temperatures were measured using a vibrating sample magnetometer equipped with a superconducting coil. The M(T) measurements were performed in the field cooled mode.

3 results and discussion

3.1. X-ray diffraction

The results of the X-ray diffraction (XRD) studies at room temperature of our samples indicate that our compounds were found to be single phase and crystallize in the orthorhombic structure with Pnma space group. Figure1 shows typical XRD patterns registered at room temperature for x = 0.1 and 0.2 samples.

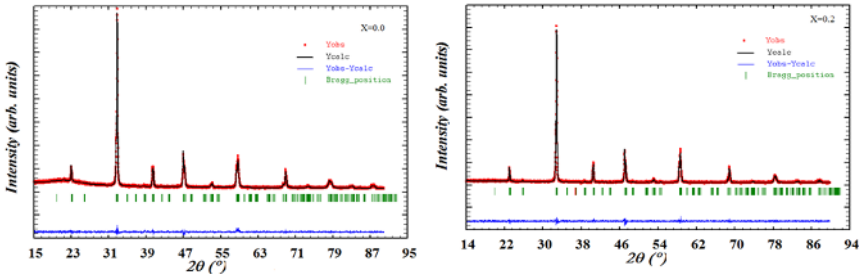

Fig.1. Observed (solid circles) and calculated (solid line) XRD patterns of the Er-doped samples (x=0.0 and x=0.2) at room temperature. The difference between these spectra is plotted at the bottom. Bragg reflections are indicated by ticks

The structural parameters are refined by Rietveld's profile- filling method. The quality of the refinement is evaluated through the goodness of the fit indicator χ^2. The structural parameters are listed in Table 1. In Figure 2 the average size of A-site cations $\langle r_A \rangle$ and the mismatch size σ^2 at the A-site are plotted. This evolution can be explained in terms of average ionic radius values; in fact, the average ionic radius of Er^{3+} (1.062 Å) is smaller than that of Pr^{3+} (1.179Å) [10, 11].

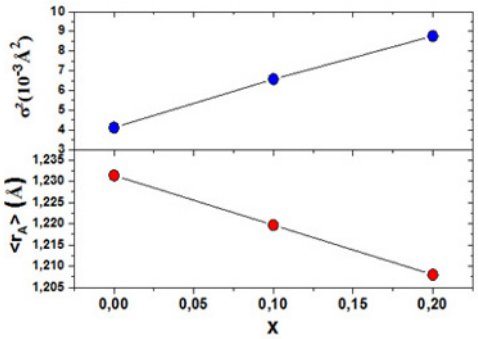

Fig.2. Average radius of the A-cation site $<r_A>$ and variance of the A-site ionic radius versus x for $Pr_{0.6-x}Er_xSr_{0.4}MnO_3$ (x=0.0, 0.1 and 0.2) samples.

Table 1*:* Refined structural parameters of $Pr_{0.6-x}Er_xSr_{0.4}MnO_3$ (x=0.0, x=0.1 and x=0.2) samples at room temperature

Parameter	x = 0.0	x = 0.1	x = 0.2
a (Å)	5.4438	5.4442	5.4415
b (Å)	7.6837	7.6846	7.6744
c (Å)	5.4723	5.4621	5.4493
V (Å^3)	228.90	228.51	227.56
Mn-O_1-Mn (°)	163.52	162.14	153.76
Mn-O_2-Mn (°)	162.72	161.2	167.4
Mn-O_1 (Å)	1.9416	1.9451	1.9701
Mn-$O_{2\text{-}I}$ (Å)	1.994	2.055	1.969
Mn-$O_{2\text{-}II}$ (Å)	1.915	1.865	1.911
χ^2	1.22	1.10	1.13

3.2. Magnetic properties

Figure 3 displays the temperature dependence of the magnetization M at a magnetic applied field of 0.05T. The M/M_{max} (T) curves do not reveal any secondary phases, which confirm the good crystallization of our samples. In the temperature range 20–300 K, a paramagnetic to ferromagnetic transition is observed. The Curie temperature T_C, which is defined as the inflection point of M (T) curve, is found to decrease from 303 K (x=0.0) to 70 K (x=0.2). Since Er^{3+} has the same valence as Pr^{3+}, the average manganese oxidation state remains constant by substitution of Er^{3+} for Pr^{3+}. The decrease of T_C can be explained by the $<r_A>$ change. In order to confirm the ferromagnetic behavior at low temperatures of our samples, we have performed magnetization measurements as a function of the magnetic applied field $\mu_0 H$ up to 7T at several temperatures. Figure 4 shows isothermal magnetization curves for x=0.1 and x=0.2. We can observe, that below T_C, the magnetization increases sharply with magnetic applied field for H<0.5T and tends to saturation above 1T.

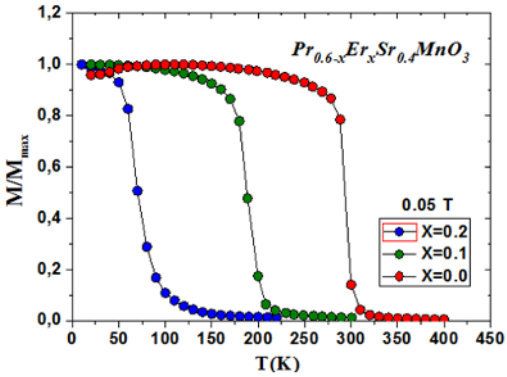

Fig. 3. $M/M_{max}(T)$ for $Pr_{0.6-x}Er_xSr_{0.4}MnO_3$ (x=0.0, x=0.1 and x=0.02) samples under 0.05 T.

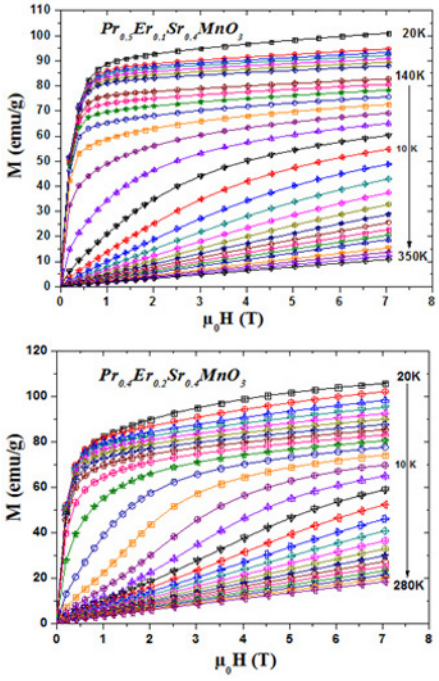

Fig.4. M (H) curves at several temperatures for $Pr_{0.6-x}Er_xSr_{0.4}MnO_3$ samples (x=0.1 and x=0.2)

3.3. Arrott curves

In order to determine the order of the magnetic phase transition for both $Pr_{0.6-x}Er_xSr_{0.4}MnO_3$ (x=0.0 and 0.1) samples, Arrott plots (M^2 vs. H/M) are plotted in Figure 5. Positive slope is observed in the Arrott plots for both x=0.0 and x=0.1 which reflects the second order phase transition. The T_C values deduced from Arrott curves (T_C corresponds to the isotherm passing through the origin) [12, 13] are very close to that obtained from the M (T) ones.

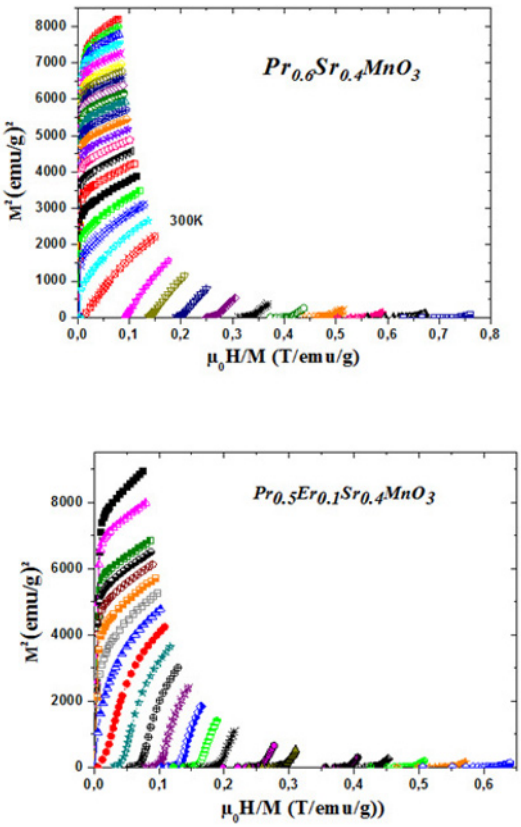

Fig.5. Arrot curves M^2 versus μ_0H/M for $Pr_{0.6-x}Er_xSr_{0.4}MnO_3$ samples (x=0.0 and x=0.1)

3.4. Magnetocaloric effect

Using the Maxwell's thermodynamic relation [14]:

$$(\frac{\partial M}{\partial T})_H = (\frac{\partial S}{\partial H})_T \quad (1)$$

The magnetic-entropy change ΔS_M, which results from the spin ordering induced by the variation of the magnetic applied field from 0 to H_{max} is given by

$$\Delta S_M(T, H_{max}) = S_M(T, H_{max}) - S_M(T, 0) = \int_0^{H_{max}} (\frac{\partial M}{\partial T})_H \, dH \quad (2)$$

For magnetization measured at discrete field and temperature intervals, the magnetic entropy change defined in Eq. (2) can be approximated by Eq.(3)[15],

$$\Delta S_M = \sum_i \frac{M_i - M_{i+1}}{T_i - T_{i+1}} \Delta H_i \quad (3)$$

The entropy change for both samples x=0.0 and x=0.1 calculated as a function of temperature at various magnetic fields is plotted in Figure 6.

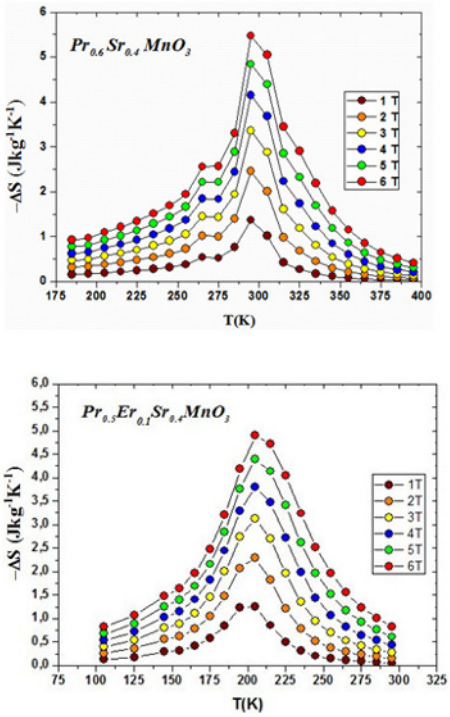

Fig.6. Magnetic entropy change versus temperature for x=0.0 and x=0.1 at various magnetic applied field changes

The maximum magnetic entropy changes observed for x = 0.0, 0.1 and 0.2 are 2.46, 2.29 and 2.4 J kg^{-1}/K^{-1}, respectively, under a magnetic field change of 2 T and reaches 4.85, 4.38 and 4.29 J kg^{-1}/K^{-1} under a magnetic field change of 5 T. The large magnetocaloric effect in perovskite manganites could originate from the spin-lattice coupling in the magnetic ordering process [16, 17]. The relative cooling power (RCP) or refrigerant capacity is a useful parameter which is deciding the efficiency of magnetocaloric materials based on the magnetic entropy change [18,19]. The estimated relative cooling power (RCP) which is computed by $RCP = -\Delta S_M(T,H) \times \delta\ T_{FWHM}$ where δT_{FWHM} is the full width at half maximum of the magnetic entropy change curve.This parameter corresponds to the amount of heat that can be transferred between the cold and hot parts of the refrigerator in one ideal thermodynamic cycle. The RCP allows for an easy comparison of different magnetic materials for applications in magnetic refrigeration; hence larger RCP values lead to better magnetocaloric materials. Our studied samples with modest values for the magnetic entropy present RCP values of 223.29, 294.46 and 315.27 J/kg at 5T for x=0.0, 0.1 and 0.2 respectively. These values are comparables although, which confirm that the larger the δT_{FWHM}, the better the cooling capacity [20]. The RCP of $Pr_{0.6-x}Er_xSr_{0.4}MnO_3$ compounds are 54.46 %, 71.81% and 76.9 % of RCP of Gd (410 J/kg) at 5T [21]. These results are interesting enough, compared with materials considered as suitable for applications in magnetic refrigerators, paving a way for investigations of materials useful for magnetic refrigeration.

4 Conclusion

The structural, magnetic and magnetocaloric properties of polycrystalline $Pr_{0.6-x}Er_xSr_{0.4}MnO_3$ (x=0.0, 0.1 and 0.2), have been investigated at high temperature. The samples were prepared by the standard ceramic process. The samples are single-phase and crystallize in the orthorhombic structure with

Pnma space group. Our compounds exhibit a paramagnetic-ferromagnetic transition with decreasing temperature. The magnetic entropy change of $Pr_{0.6-x}Er_xSr_{0.4}MnO_3$ has been studied. The maximum of the magnetic entropy change is found to be 4.85, 4.38 and 4.29 J kg^{-1}/K^{-1} for x = 0.0, 0.1 and 0.2 respectively, under a magnetic field change of 5 T. Our samples exhibit high RCP values of 223.3, 294.5 and 315.3 J/kg at 5T for x=0.0, 0.1 and 0.2 respectively.

Acknowledgment

This study was supported by the Tunisian Ministry of Higher Education and Scientific Research.

References

1. E. Dagotto, T. Hotta and A. Moreo, *Physical Reports* **344**, 1 (2001).
2. C. Zener, Phys. Rev. **82** 403 (1951).
3. A. J. Millis, P. B. Littlewood , B. J. Shraiman, Phys. Rev. Lett. **74**, 5144 (1995).
4. E. Pollert, Z. Jirák, J. Hejtmánek, A. Strejc, R. Kužel, V. Hardy. J. Magn. Magn. Mater. **246,** 290 (2002).
5. T. Wu, M. Mitchell. Phys. Rev. B, **69,** 100405 (2004).
6. S. Hebert, A. Maignan, V. Hardy, C. Martin, M. Hervieu, B. Raveau, R. Mahendiran, P. Schiffer. Eur. Phys. J. B **29,** 419 (2002).
7. R. Mahandiran, A. Maignan, S. Hebert, C. Martin, M. Hervieu, B. Raveau, J.F. Mitchell and P. Schiffer. Phys. Rev. Lett. **89,** 286602 (2002).
8. H. M. Rietveld, J. Appl. Cryst, **2**, 65 (1969).
9. J. Rodriguez-Carvajal, Physica B **192**, 55 (1993). For more details on the FULLPROF Suite of programs consult the site: http://www.ill.eu/sites/fullprof/
10. R. D. Shannon, C. T. Prewitt, Acta Cryst. B **25**, 925 (1969).
11. R. D. Shannon, C. T. Prewitt, Acta Cryst. B **26**, 1046 (1970).
12. A. Arrott, J. E. Noakes, Phys, Rev. Lett. **19,** 786 (1967).
13. S. K. Banerjee, Phys. Lett. **12,** 16 (1964).
14. A. H. Morrish, *The Physical Principles of Magnetism*, Wiley, New York, (Chapter 3), (1965).
15. M. Foldeaki, R. Chahine, T. K. Bose, J. Appl. Phys. **77,** 3528 (1995).
16. M. H. Phan, S. C. Yu, N. H. Hur, Y. H. Yeong, J. Appl. Phys. **96,** 1154 (2004).
17. P. G. Radaelli, D. E. Cox, M. Marezio, S. W. Cheong, P. E. Schiffer, A. P. Ramirez, Phys. Rev. Lett. **75,** 4488 (1995).
18. V. K. Pecharsky, K.A. Gschneidner, A.O. Tsokol, Rep. Prog. Phys. **68** 1479 (2005).
19. K. A. Gschneidner Jr., V. K. Pecharsky, Annu. Rev. Mater. Sci. **30** 387 (2000).
20. V. K. Pecharsky and K. A. Gschneidner Jr., Phys. Rev. Lett. **78** 4494 (1997).
21. M. H. Phan, S. C. Yu, J. Magn. Magn. Mater. **306** 325 (2007).